Biosensors and Bioelectronics 79 (2016) 701–708

Contents lists available at ScienceDirect

Biosensors and Bioelectronics

journal homepage: www.elsevier.com/locate/bios

Development of a highly specific and sensitive cadmium and lead microbial biosensor using synthetic CadC-T7 genetic circuitry

Hyun Ju Kim [a,b,1], Ji Won Lim [c,1], Haeyoung Jeong [b,d], Sang-Jae Lee [e], Dong-Woo Lee [f], Taesung Kim [c,g,*], Sang Jun Lee [a,b,**]

[a] Infection and Immunity Research Center, Korea Research Institute Bioscience and Biotechnology (KRIBB), Daejeon, Republic of Korea
[b] Biosystems & Bioengineering Program, University of Science and Technology (UST), Daejeon, Republic of Korea
[c] Department of Biomedical Engineering, Ulsan National Institute of Science and Technology (UNIST), Ulsan, Republic of Korea
[d] Superbacteria Research Center, KRIBB, Daejeon, Republic of Korea
[e] Department of Bio-Food Materials, Silla University, Busan, Republic of Korea
[f] School of Applied Biosciences, Kyungpook National University, Daegu, Republic of Korea
[g] Department of Mechanical Engineering, UNIST, Ulsan, Republic of Korea

ARTICLE INFO

Article history:
Received 11 October 2015
Received in revised form
8 December 2015
Accepted 29 December 2015
Available online 29 December 2015

Keywords:
CadC
Heavy metal ions
Microbial biosensor
Microfluidic device
T7 RNA polymerase

ABSTRACT

Multiple copies of a *cadC* homolog encoding a heavy metal-responsive transcription factor were found in the genome of a bacterium isolated from ocean sediment, and the heavy metal responses of the encoded proteins were characterized using a fluorescence reporter assay. Each CadC regulator exhibited distinct specificity in response to heavy metal ions, indicating their potential use as modular heavy metal biosensors. Next, we constructed CadC-controlled T7 RNA transcription systems for intracellular signal amplification, i.e., higher sensitivity. Flow cytometry revealed that cadmium and lead ions could be recognized specifically by CadC-T7 biosensors, which could be combined with a microfluidic platform to generate heavy metal biosensor devices with increased sensitivity. Our results demonstrate the successful development of synthetic CadC-T7 genetic circuitry for use in improved heavy metal biosensor microfluidic devices.

1. Introduction

Accumulation of heavy metals, which are ubiquitous in our environment, sometimes causes serious pollutions of water, soil, and air (Azarbad et al., 2013). Harmful heavy metals such as arsenic, cadmium, chromium, mercury, and lead pose risks to human health (Jaishankar et al., 2014). In particular, heavy metals can cause many fatal diseases such as cancer, nerve disorders, and kidney failure, mostly via oxidative stress resulting from metal-induced reactive oxygen species (Cuypers et al., 2010; Ercal et al., 2001).

Nanomolar concentrations of heavy metal ions can be detected sensitively by analytical techniques such as inductively coupled plasma/mass spectrometry (ICP/MS) and atomic absorption spectrometry (AAS) (Steven et al., 1996). However, these methods have disadvantages, including high cost, technical difficulty, time-consuming sample preparation, and the inability to perform multiplex analyses; therefore, biosensors such as enzymes and antibodies have been developed to address these weaknesses (Bereza-Malcolm et al., 2015). Notably, a highly sensitive fluorescence immunoassay capable of detecting nanomolar concentrations of cadmium ions has been developed (Blake et al., 2001).

Recently, whole-cell microbial biosensors were developed to detect various toxic metal ions (Lei et al., 2006). The regulatory elements of heavy metal resistance operons isolated from several bacterial strains have been harnessed to construct bacterial biosensors for heavy metals such as cadmium and lead (Raja and Selvam, 2011; Shetty et al., 2003). Recently, whole cell-based cadmium sensors have been optimized by altering CadR specificity (Tao et al., 2013) or by coupling to a genetic circuit that functions as a toggle (Wu et al., 2009).

Various types of genetic circuit, including genetic amplifiers, have been designed to program cellular responses and to precisely control genetic networks (Sayut et al., 2007). For example, the LuxR-based positive-feedback amplifier increases sensitivity to the input signal and intensifies the output signal (Nistala et al., 2010).

* Corresponding author at: Department of Mechanical Engineering, Ulsan National Institute of Science and Technology (UNIST), 50 UNIST-gil, Ulsan 44919, Republic of Korea.
** Corresponding author at: Infection and Immunity Research Center, Korea Research Institute of Bioscience and Biotechnology (KRIBB), 125 Gwahak-ro, Yuseong-gu, Daejeon 34141, Republic of Korea.
E-mail addresses: tskim@unist.ac.kr (T. Kim), leesj@kribb.re.kr (S.J. Lee).
[1] These authors contributed equally to this work.

http://dx.doi.org/10.1016/j.bios.2015.12.101
0956-5663/

A recent study showed that a genetic AND gate can function as a genetic filter as well as a genetic amplifier (Wang et al., 2013). In addition to genetic circuits, various tools have been designed to develop heavy metal biosensors. For example, an *E. coli* sensor set was used in conjunction with binary regression models (Hou et al., 2015) and flow-cytometric analysis (Hurdebise et al., 2015) to specifically detect bioavailable heavy metals.

Over the past decade, micro/nanotechnologies have been integrated with microbial biosensors to enable minimization of sample and reagent volumes, rapid high resolution and high-throughput analyses, high reproducibility, and high portability (Hegab et al., 2013; Lim et al., 2015). Recently, microfluidic devices have been combined with microbial biosensors to enable sensitive detection of heavy metal ions and toxic compounds (Gammoudi et al., 2010; Garcia-Alonso et al., 2009); for the same purpose, we also developed a chemostat-like microfluidic platform (Kim et al., 2014). In this study, we determined heavy metal specificities of CadC transcriptional regulators that were repeatedly found in the genome of *Bacillus oceanisediminis* 2691 (Lee et al., 2012). Further, we selected and recombined synthetic modules including promoters, operators, and regulators derived from CadC and T7 transcription systems to create highly specific CadC-controlled T7 RNA polymerase circuits that are capable of detecting trace amounts of cadmium and lead ions in a microfluidic platform.

2. Experimental

2.1. Plasmid and strains

The bacterial plasmids and strains constructed for this study are listed in the Table 1, and described in detail in supplementary Figs. S1 and S2. Six *cadC* homologs, including their original promoters, were transcriptionally fused upstream of the *egfp* reporter gene to generate prototype pCadC plasmids (pCadC538, pCadC551, pCadC595, pCadC640, pCadC1945, and pCadC4657). Modular fusions of *cadO–egfp* under the control of the T7 promoter (P_{T7}–*cadO–egfp*) were constructed on the backbone of a pET21a(+) Δ*lacI* plasmid to generate six pT7cadO plasmids: pT7cadO538, pT7cadO551, pT7cadO595, pT7cadO640, pT7cadO1945, and pT7cadO4657. In addition, six *cadC* overexpression modules (P_{hce}–*cadC*) were inserted into the pT7cadO plasmids to generate pT7cadO-H plasmids (Fig. S1). For chromosomal construction, six *cadC* genes were placed upstream of the T7 RNA polymerase gene in the BL21(DE3) Δ*lacI* strain, ultimately yielding strains HK757, HK758, HK759, HK760, HK744, and HK739 (Fig. S2).

Table 1
Plasmids and *E. coli* strains constructed in this study.

Plasmid or *E. coli* strain	Relevant characteristics
Plasmid	
pCadC538	*cadC*538–*egfp* in T-Blunt™
pCadC551	*cadC*551–*egfp* in T-Blunt™
pCadC595	*cadC*595–*egfp* in T-Blunt™
pCadC640	*cadC*640–*egfp* in pJET1.2
pCadC1945	*cadC*1945–*egfp* in T-Blunt™
pCadC4657	*cadC*4657–*egfp* in T-Blunt™
pT7cadO538	P_{T7}–*cadO*538–*egfp* in pET21a(+) Δ*lacI*
pT7cadO551	P_{T7}–*cadO*551–*egfp* in pET21a(+) Δ*lacI*
pT7cadO595	P_{T7}–*cadO*595–*egfp* in pET21a(+) Δ*lacI*
pT7cadO640	P_{T7}–*cadO*640–*egfp* in pET21a(+) Δ*lacI*
pT7cadO1945	P_{T7}–*cadO*1945–*egfp* in pET21a(+) Δ*lacI*
pT7cadO4657	P_{T7}–*cadO*4657–*egfp* in pET21a(+) Δ*lacI*
pT7cadO538-H	pT7cadO538 plus P_{hce} –*cadC*538
pT7cadO551-H	pT7cadO551 plus P_{hce} –*cadC*551
pT7cadO595-H	pT7cadO595 plus P_{hce} –*cadC*595
pT7cadO640-H	pT7cadO640 plus P_{hce} –*cadC*640
pT7cadO1945-H	pT7cadO1945 plus P_{hce} –*cadC*1945
pT7cadO4657-H	pT7cadO4657 plus P_{hce} –*cadC*4657
E. coli strain	
HK730	BL21(DE3) Δ*lacI*::FRT-Km^R-FRT
HK731	BL21(DE3) Δ*lacI*::FRT
HK757	*cadC*538–T7 RNAP (Km^R) in the genome of HK731
HK758	*cadC*551–T7 RNAP (Km^R) in the genome of HK731
HK759	*cadC*595–T7 RNAP (Km^R) in the genome of HK731
HK760	*cadC*640–T7 RNAP (Km^R) in the genome of HK731
HK744	*cadC*1945–T7 RNAP (Km^R) in the genome of HK731
HK739	*cadC*4657–T7 RNAP (Km^R) in the genome of HK731

2.2. Fluorescence measurement

Single colonies of *E. coli* DH5α (Solgent, Daejeon, Korea) harboring *cadC–egfp* plasmids (pCadC538, pCadC551, pCadC595, pCadC640, pCadC1945, or pCadC4657) were grown overnight at 37 °C in LB media supplemented with 50 μg/mL ampicillin. The overnight cultures were diluted 100-fold in 100 mL of fresh LB medium supplemented with 50 μg/mL ampicillin and incubated at 37 °C in a 500 mL flask with shaking at 180 rpm until the OD_{600} reached 0.4. Various heavy metal chemicals (final concentrations: 0, 5, 10, 25, 50, and 100 μM) were added to 4 mL aliquots of bacterial culture in 15 mL test tubes. After incubation at 37 °C for 2 h, optical densities (OD_{595}) and fluorescence intensities (FI) were measured using a TECAN Infinite 2000 plate reader (excitation 485/20 nm; emission 535/25 nm; gain=40, top reading) and TECAN i-Control software (TECAN, Salzburg, Austria). Due to the variable basal level expressions of microbial constructs with *cadC–egfp* and P_{T7}–*cadO–egfp*, specific changes in fluorescence intensity [$\Delta F/\Delta OD = (FI_{2h} - FI_{0h})/(OD_{2h} - OD_{0h})$] were calculated.

Various concentrations of cadmium and lead were added to cultures of *E. coli* HK760 cells carrying the pT7cadO640-H plasmid and to HK744 cells carrying the pT7cadO1945 plasmid and specific changes in fluorescence intensity (ΔF/ΔOD) were measured and calculated as described above.

2.3. Flow cytometry

E. coli cells of strains HK757, HK758, HK759, HK760, HK744, and HK739 (*cadC*–T7 RNA polymerase in genome) carrying pT7cadO (P_{T7}–*cadO–egfp*) or pT7cadO-H (P_{T7}–*cadO–egfp* plus P_{hce}-*cadC*) were grown in the same manner as described above, and arsenite, cadmium, lead, and zinc heavy metal ions (final concentration, 30 μM) were added. To observe cell populations on the cellular level, a flow cytometer Cube 6 system (Partec, Münster, Germany) was used. The flow cytometer was equipped with a 488 nm blue solid-state laser. Fluorescence intensity was detected on fluorescence channel FL1 at 527 ± 15 nm. Culture samples were diluted 100-fold to obtain 10^5 counts below 5,000 particles/s, and the flow was 1 μL/s during measurement mode.

2.4. Microfluidic platform

We used the chemostat-like microfluidic platform described in our previous work (Kim et al., 2014) to quantitatively compare the sensitivity and performance of the prototype and CadC-T7 microbial sensors. Therefore, the microfluidic channel network was the same as before, and fabricated in exactly the same manner using standard photolithography technology, including soft lithography. Overnight-cultured cells suspended in tryptone broth (TB) media (1% tryptone and 0.5% NaCl) containing the corresponding heavy metal ions were initially loaded such that ten cells occupied each microfluidic chamber, and the chemical culture environment was maintained to facilitate the expression of reporter genes during cellular growth. The microfluidic platform was then placed in an incubator (60% humidity, 37 °C) on top of a microscope stage.

Optical and fluorescence micrographs were acquired every 2 h using an inverted epi-fluorescence microscope (Ti-U, Nikon, Tokyo,

Japan) equipped with a CCD camera (ORCA R2, Hamamatsu Photonics, Hamamatsu, Japan). The fluorescence intensities from the micrographs were analyzed using ImageJ (NIH, Bethesda, MD, USA).

3. Results and discussion

3.1. Mining of cadC and cadO bio-parts

The initially identified *cadCA* operon of *Staphylococcus aureus* plasmid pI258 confers microbial resistance to divalent cadmium, lead, and zinc ions (Endo and Silver, 1995; Sun et al., 2001). The *cadCA* operon consists of the *cadC* gene, encoding metal-sensing transcriptional regulators, and the *cadA* gene, encoding heavy metal efflux pumps (Fig. 1A). The *cadO* operator is located upstream of the *cadC* gene to allow auto-regulation of P_{cadC} promoter activity by CadC regulators. In the genome sequence of *B. oceanisediminis* 2691 (Lee et al., 2012), we found six *cadC* homologs encoding DNA binding transcription factors, five of which (*cadC*538, *cadC*595, *cadC*640, *cadC*1945, and *cadC*4657) are adjacent to genes encoding putative heavy metal-transporting ATPases (CadA); the exception was *cadC*551.

By comparing these genes to the *cadO* operator from pI258, six *cadO* DNA sequences ($ANTCAAN_8TTGANT$) were identified (Fig. 1B). The deduced amino acid sequences of six *cadC* homologous genes were similar to one another. In addition, the heavy metal binding motifs (Ye et al., 2005) in CadC proteins were highly conserved (Fig. 1C). For example, cysteine residues at positions 7, 11, 58, and 60 in the deduced sequences of CadC proteins were perfectly conserved relative to CadC derived from pI258, and Asp101, His103, His114, and Lys117 were also completely conserved except in CadC551.

We anticipated that these *cadO* operators and CadC regulators can be combined to regulate the expression of *cadCA* operons in response to the presence of intracellular heavy metal ions. The expression of *cadC* genes in *B. oceanisediminis* 2691 was monitored using RT-PCR after the addition of various concentrations (final 0, 10, 30, and 100 μM) of heavy metals to the culture medium when the OD_{600} reached 0.6. The relative transcript levels in induced

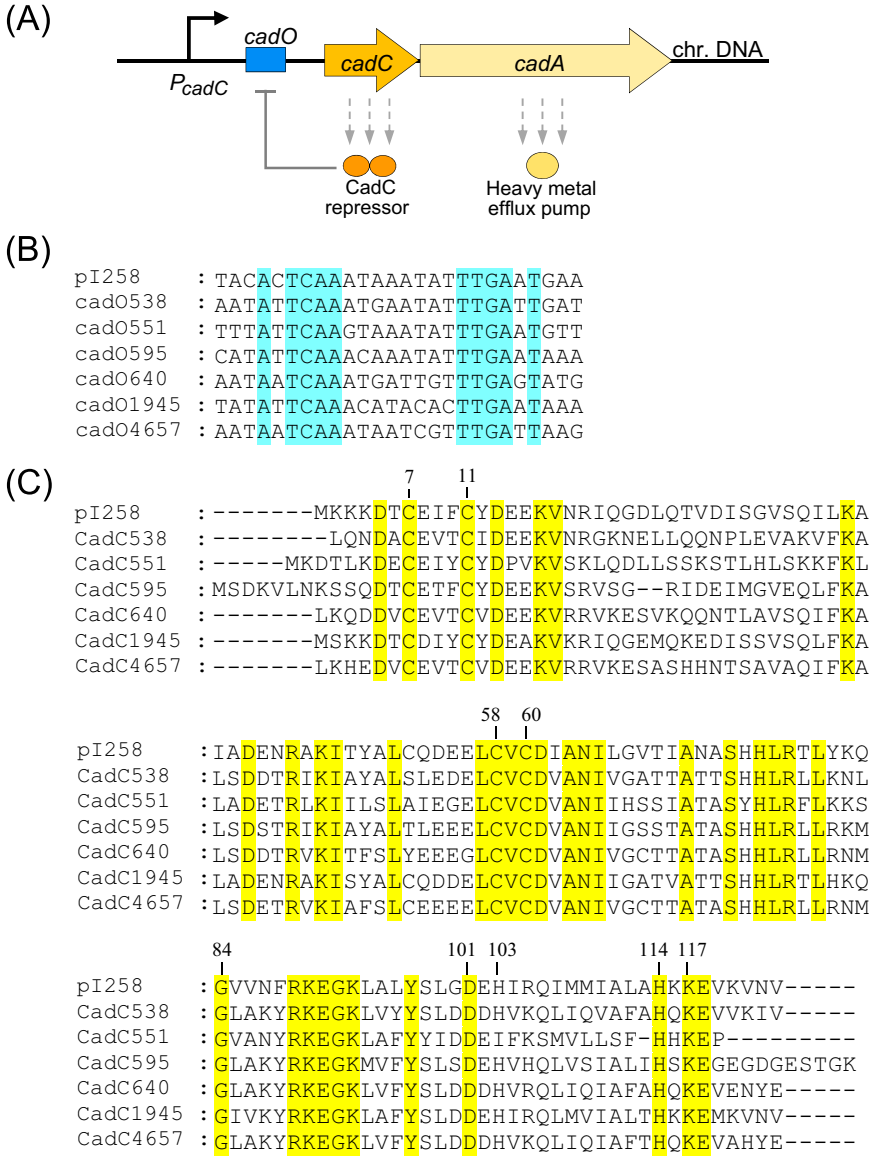

Fig. 1. *cadC* homologs in the genome of *B. oceanisediminis* 2691. (A) Structure of the *cadCA* operon in *Staphylococcus aureus* plasmid pI258. (B) Multiple sequence alignment of *cadO* nucleotide sequences. (C) Multiple sequence alignment of CadC proteins. Completely conserved nucleotides and amino acids are shaded in blue and yellow, respectively.

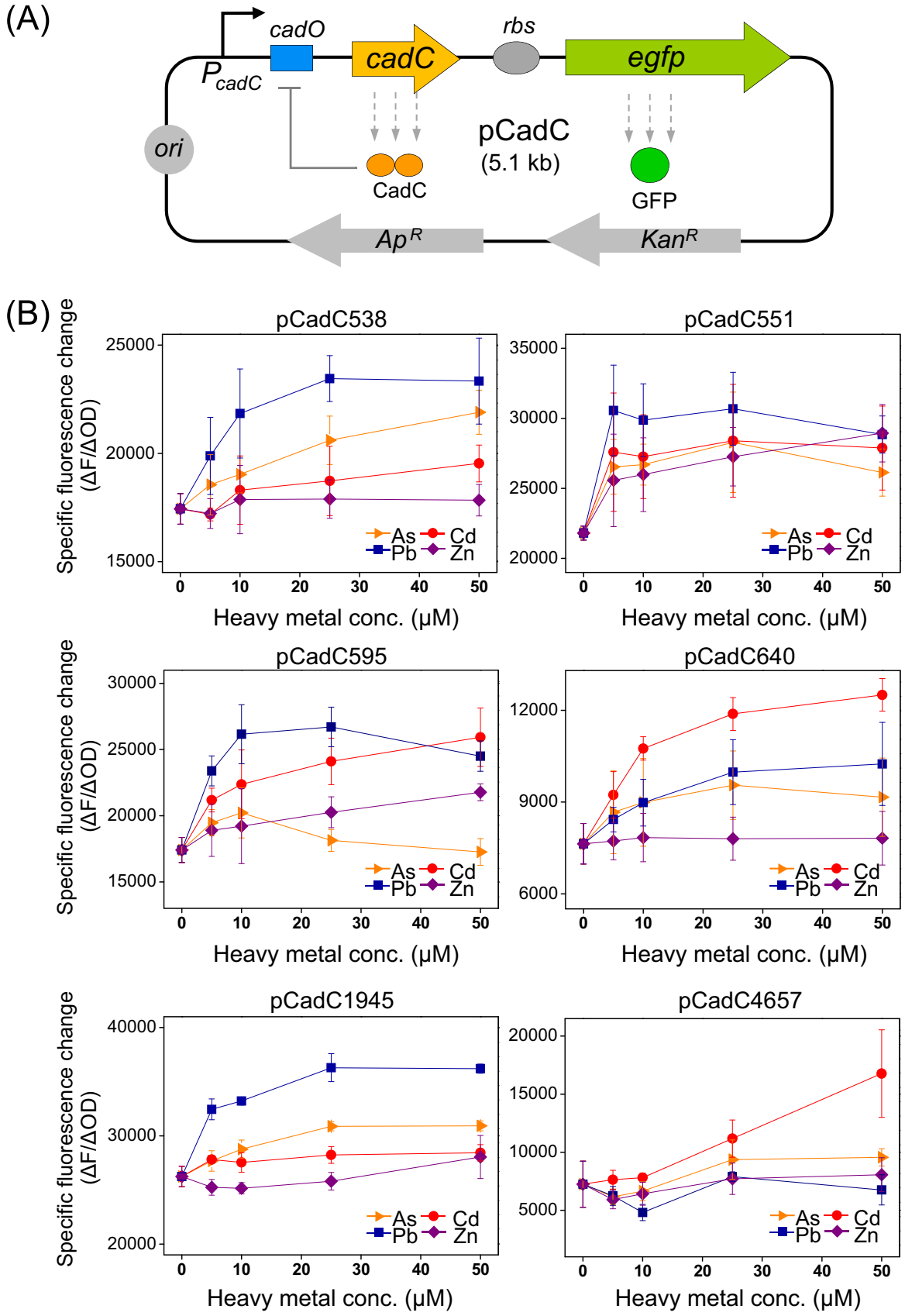

Fig. 2. Identification of heavy metal specificities of CadC transcription factors. (A) Construction of *cadC–egfp* transcriptional fusions in plasmid pCadC. (B) Concentration-dependent heavy metal responses of prototype biosensors (recombinant *E. coli* DH5α carrying six pCadC plasmids).

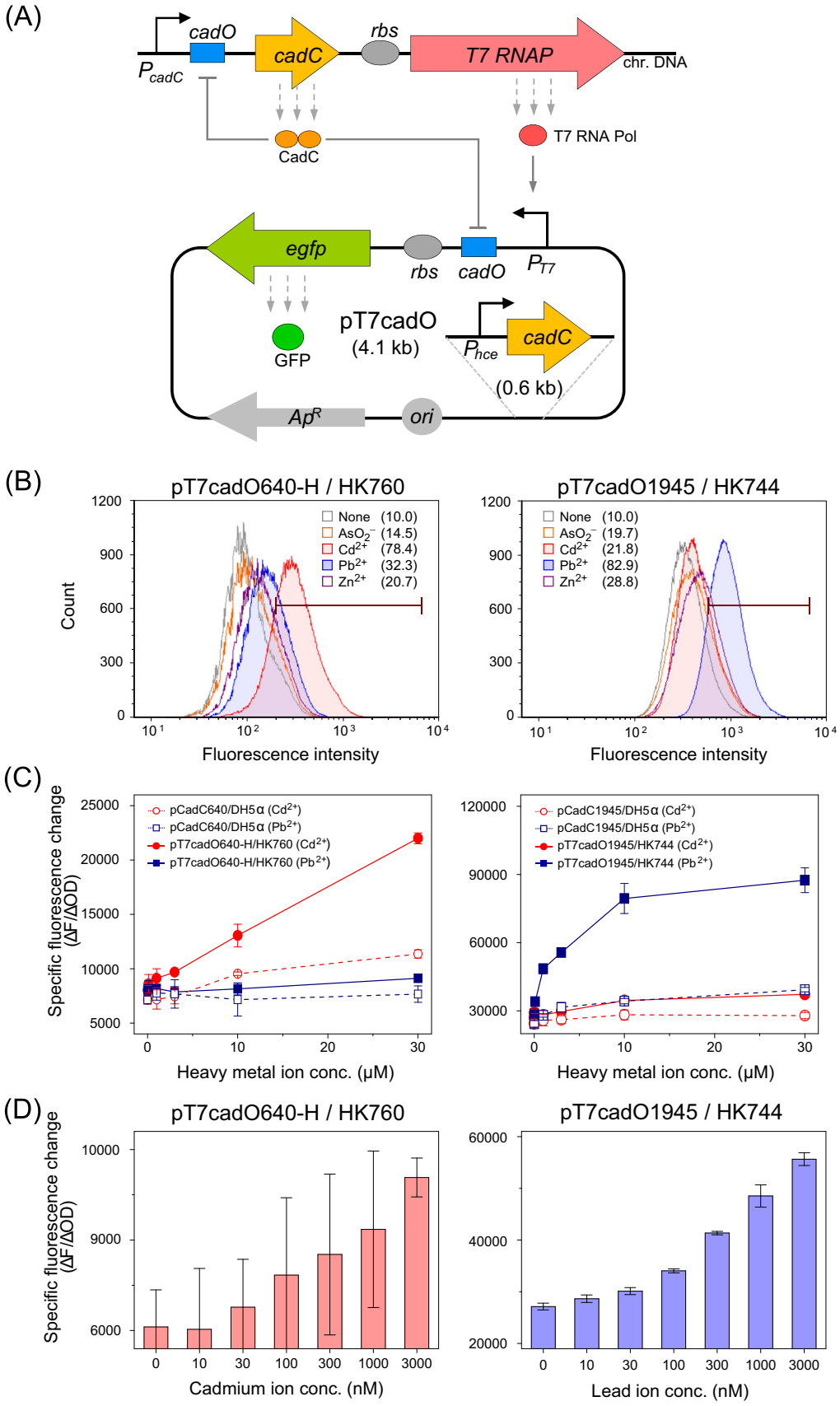

Fig. 3. Improved heavy metal microbial biosensors carrying CadC-T7 synthetic circuits. (A) Construction of synthetic CadC-controlled T7 signal amplification circuits. (B) Flow-cytometric profiles of cadmium and lead microbial biosensors. (C) Comparison of specific fluorescence changes generated by prototype biosensors, DH5α carrying pCadC640 or pCadC1945 plasmid, and upgraded microbial biosensors with CadC-T7 circuits at different concentrations of heavy metals. (D) Detection limits of cadmium and lead ions of CadC-T7 biosensors, HK760 carrying pT7cadO640-H, and HK744 carrying pT7cadO1945.

versus non-induced cultures are shown in Fig. S3. Transcription of the *cadC*538, *cadC*595, *cadC*640, *cadC*1945, and *cadC*4657 genes was induced by cadmium ions in a concentration-dependent manner, and *cadC*1945 and *cadC*4657 genes was induced by high concentrations of lead ions; however, the expression of *cadC*551 genes was less responsive to cadmium and lead ions than that of other *cadC* genes. Arsenite and zinc ions induced only marginal expression of *cadC* genes (Fig. S3).

These results indicated that CadC is more highly responsive to cadmium and lead ions than to arsenite and zinc ions. However, due to possible cross-reactivity between several *cadO* operators and CadC transcription factors in the original microbial cells, we chose to further characterize the specificity and inducibility of each CadC regulator in recombinant *E. coli* cells.

3.2. Heavy metal specificity of CadC transcription factors

To identify the ligand specificity of CadC proteins, recombinant transcriptional fusions of *cadC* and *egfp* genes were constructed in *E. coli*. The *cadA* gene, located downstream of the *cadC* gene in the *cadCA* operon, was replaced by the *egfp* gene so that a GFP reporter could be controlled by the authentic *cadC* promoter and *cadO* operator (Fig. 2A). Six different *cadC*–*egfp* transcriptional reporter plasmids were constructed: pCadC538, pCadC551, pCadC595, pCadC640, pCadC1945, and pCadC4657 (Table 1). Recombinant *E. coli* DH5α carrying six different plasmids were grown, and metal specificities were monitored. Excess levels of 14 different kinds of heavy metals (final, 100 μM) were added to the culture of recombinant *E. coli* cells.

E. coli harboring pCadC538 exhibited a significant response to cadmium (Fig. S4). Similarly, recombinant cells harboring pCadC640 or pCadC4657 also responded highly to cadmium. *E. coli* carrying pCadC551 did not react with any of the heavy metals tested, consistent with the results of transcriptional analysis of *cadC*551 gene in *B. oceanisediminis* 2691 (Fig. S3). Cells carrying pCadC595 are highly responsive to cadmium and lead, and slightly to arsenite. Lead ions highly activated the transcription of the *cadC*1945–*egfp* construct, and arsenite, and cadmium ions activated the transcription of *egfp* under the control of the *cadC*1945 gene.

3.3. Prototype biosensors with heavy metal-responsive CadC regulators

Based on the heavy metal specificities of CadC proteins, cadmium, lead, arsenite, and zinc were selected for further characterization of the specificities of CadC transcription factors (Fig. 2B). To this end, different concentrations of four heavy metals were added to the cultures of recombinant *E. coli* harboring pCadC plasmids in order to measure specific fluorescence changes after 2 h of further incubation. Cells carrying plasmids pCadC538, pCadC595, and pCadC1945 were highly responsive to lead ions. Half-maximal concentrations of lead ions as inducers of the CadC538, CadC595, and CadC1945 transcription factors were around 5 μM. *E. coli* carrying pCadC551 exhibited wide variations in all concentration ranges examined. Two highly cadmium-responsive cells, those carrying pCadC640 or pCadC4657, were identified. Cells harboring pCadC640 were more sensitive to cadmium ions at lower concentrations than cells carrying pCadC4657.

In the cases of arsenite and zinc ions, recombinant reporter cells responded only slightly or poorly at lower concentrations. Reportedly, Gly84 in CadC is responsible for the lack of regulation by zinc ions (Kandegedara et al., 2009). We observed that the Gly84 residue was completely conserved in CadC proteins (Fig. 1C), potentially explaining why zinc ions cannot induce the transcription of *cadC* genes in both *B. oceanisediminis* 2691 and *E. coli* cells. In addition, CadC551 did not respond to any of the heavy metals at high concentration (100 μM), probably due to its shorter C-terminus and/or lack of His103, which is responsible for CadC dimerization (Ye et al., 2005).

These data indicate that prototype biosensors using six recombinant CadC proteins had different heavy metal preferences and sensitivities to cadmium and lead ions. These biosensors could be used as modules in synthetic genetic circuits with relevant specificities.

3.4. Synthetic CadC-controlled T7 signal amplification systems for whole-cell biosensors

Next, we harnessed T7 transcription modules to address the wide variations and low fluorescence signals in our *cadC*–*egfp* prototype constructs in the *E. coli* system. In the presence of heavy metal ions in cells, T7 RNA polymerase (T7 RNAP) was expressed, and the T7 promoter was activated (Fig. 3A). For several decades, T7 RNAP transcription systems have been widely used for the specific overexpression of heterologous proteins in *E. coli* (Dubendorff and Studier, 1991; Studier, 2014), yeasts (Hobl et al., 2013), and plants (Nguyen et al. 2004); these systems were designed to eliminate modular interference in cells. Recently, engineered orthogonal T7 RNA polymerases have been used for modular control of multiple pathways (Segall-Shapiro et al., 2014; Temme et al., 2012).

The T7 RNAP gene was placed downstream of *cadC* genes, under the control of *cadC* promoters. The *cadC*–T7 RNAP synthetic modules were constructed in the chromosome of *E. coli* BL21(DE3) Δ*lacI*. Next, an *egfp* reporter gene was placed under the control of the T7 promoter in a plasmid, in which the *cadO* operator and P_{hce}–*cadC* overexpression modules were inserted for tight control (Fig. S1). Ultimately, we constructed 12 pT7CadO and pT7CadO-H plasmids (Table 1) and completed six chromosomal constructs (Fig. S2).

Twelve different strains were constructed and grown after transformation of 12 plasmids (pT7cadO and pT7cadO-H) into the corresponding six *cadC*–T7 RNAP strains, and their heavy metal-responsive population changes were monitored using flow cytometry (Fig. S5). P_{hce}–*cadC* overexpression modules were not required for proper responses to heavy metals in two strains (HK758 carrying pT7cadO551 and HK744 carrying pT7cadO1945). In the case of three strains (HK759 carrying pT7cadO595-H, HK760 carrying pT7cadO640-H, and HK739 carrying pT7cadO4657-H), P_{hce}–*cadC* overexpression modules were necessary for significant responses. This difference might be due to the different DNA binding affinities of *cadO* operators and CadC proteins. Unfortunately, HK757 cells carrying pT7cadO538 were not responsive to any of the heavy metals tested, and their flow-cytometric profile was not improved by the presence of the P_{hce}–*cadC* overexpression module.

Based on flow-cytometric experimental profiles, we selected two strains, HK760 carrying pT7cadO640-H, and HK744 carrying pT7cadO1945 (Fig. S5). Marker ranges were fixed in flow-cytometric profiles such that 10% of non-treated cells fell within the range. In the case of pT7cadO640-H/HK760, 78.4% of the cellular population exhibited higher fluorescence intensity in response to cadmium ions (final, 30 μM), whereas 32.3% of total cells were shifted into the marker range when lead ions were administered. In the case of pT7cadO1945/HK744, 82.9% of cells were shifted into the marker range in response to lead ions (final, 30 μM), whereas 21.8% of total cells were found in the marker range when cadmium ions were added (Fig. 3B). These data showed that pT7cadO640-H/HK760 (*cadC*640–T7) and pT7cadO1945/HK744 (*cadC*1945–T7) were specifically responsive to cadmium and lead ions, respectively.

At various concentrations (< 30 μM) of lead and cadmium ions, specific fluorescence changes in the *cadC*640–T7 and *cadC*1945–T7 systems were dramatically increased in a concentration-dependent manner (Fig. 3C). The *cadC*640–T7 system exhibited a linear correlation between cadmium concentrations and specific fluorescence changes. In the case of the CadC1945–T7 system, the concentration of lead ions (around 5 μM) required for half-maximal induction was unchanged, when compared with that of the pCadC1945 prototype system (Fig. 2B and Fig. 3C). At 30 μM cadmium and lead ions, the specific fluorescence change values of the *cadC*640–T7 and *cadC*1945–T7 systems were 1.9- and 2.6-fold higher than those of prototype biosensors carrying pCadC540 and pCadC1945, respectively.

The *cadC*1945–T7 system could detect lead ions at a concentration of 10 nM; however, the *cadC*640–T7 system detected cadmium ions with wide variations at lower concentrations (< 3 μM) (Fig. 3D). In addition, we compared CadC-T7 whole-cell biosensors with conventional ICP methods by testing unknown samples (Table S1). We calculated the concentration of heavy metals in the samples from specific changes in fluorescence (ΔF/ΔOD) based on regression curves generated from the CadC-T7 system (Fig. S6). These data showed that the *cadC*1945-T7 biosensor is more reliable for detecting lower concentrations of lead ions, and that the *cadC*640-T7 biosensor can detect a wider range of cadmium ion concentrations.

3.5. *Microbial sensors combined with a microfluidic platform*

Using a chemostat-like microfluidic platform (Kim et al., 2014), we investigated the sensitivity of four recombinant constructs: pT7cadO640-H/HK760 and pCadC640/DH5α for cadmium detection, and pT7cadO1945/HK744 and pCadC1945/DH5α for lead detection. Fluorescence intensities were measured every 2 h via quantitative analysis of microscopic images from cells grown in the presence of various concentrations of cadmium and lead ions (negative control, 2 nM, 200 nM, and 20 μM). The relative fluorescence intensities over a time course are presented in Fig. 4. The relative fluorescence intensities of the CadC-T7 module-mediated constructs (i.e., pT7cadO640-H/HK760 and pT7cadO1945/HK744) were much stronger than those of the prototype biosensors (i.e., pCadC640/DH5α and pCadC1945/DH5α) with regard to the detection of both cadmium and lead ions, which can be explained by faster growth of BL21(DE3) derivatives and higher expression of green fluorescent proteins.

In test tube cultures, the heavy metal sensitivity of CadC-T7 microbial sensors capable of detecting cadmium and lead ions increased by 1.9- and 2.6-fold, respectively (Fig. 3C). The microfluidic platform dramatically improved the sensitivities of CadC-T7 systems relative to prototype biosensors (e.g., 15.0- and 9.2-fold increases for cadmium and lead ions, respectively, at 20 μM after 10 h). In addition, a wide range of concentrations (2 nM to 20 μM) of cadmium and lead ions could be detected in parallel in the microfluidic microbial biosensor device. This result can be attributed to the proper operation of synthetic T7 amplification genetic circuits (i.e., pT7cadO640-H/HK760 and pT7cadO1945/HK744) in the microfluidic device.

Although we observed wider variations in specific fluorescence intensity changes in response to cadmium ions (< 3 μM) in pT7cadO640-H/HK760 sensors grown in test tubes (Fig. 3D), we observed stabilized fluorescence intensities at lower concentrations of cadmium ions (Fig. 4A). It is unclear why microbial sensors were stabilized in the microfluidic relative to the test tube conditions. One contributing factor might be the continuous supply of fresh nutrients plus heavy metal ions to the cells, with the aid of the chemostat-like function of the microfluidic platform; such an explanation would be consistent with our previous work (Kim et al., 2014). From a practical point-of-view, the removal of biological growth inhibitors should be considered when pretreating samples. While the time taken for bacteria to grow is a weakness of whole cell-based sensors, the portability and multiplex advantages of microfluidic microbial biosensors will facilitate the development of high-throughput, and low-cost instrumentation for multiple on-site analyses.

4. Conclusion

In the synthetic biology era, biological parts and modules with relevant functions can be excavated from enormous genomic and metagenomic sequence databases, and then reassembled to

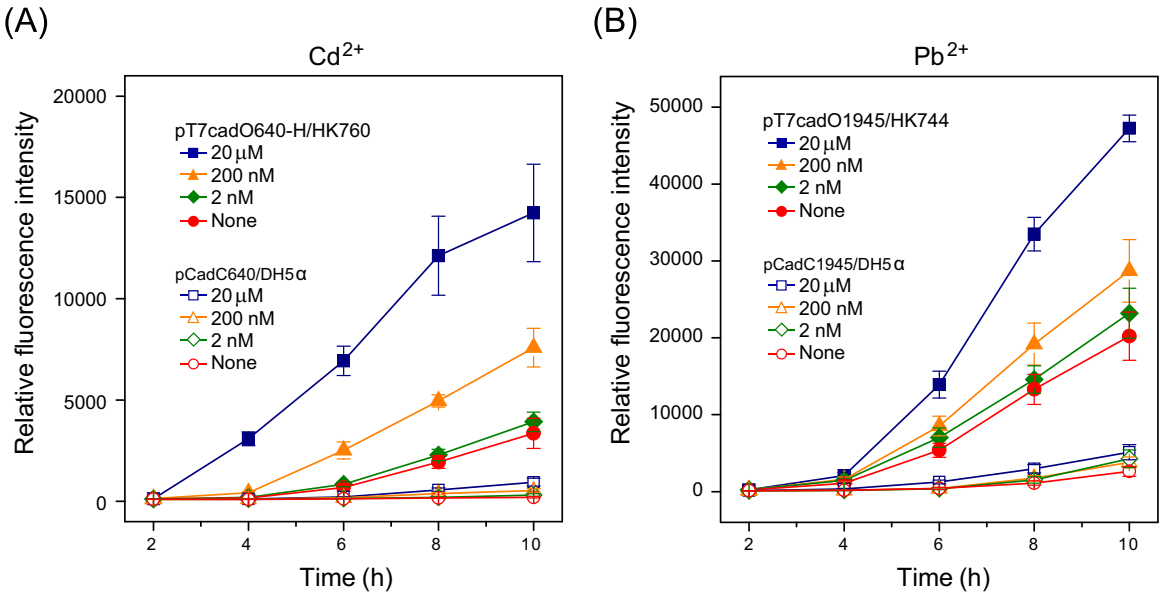

Fig. 4. Detection of heavy metal ions by the microfluidic biosensor device. Time-course quantification of fluorescence intensities generated by *E. coli* cells grown in microfluidic chambers. Fresh nutrients with (A) lead and (B) cadmium ions were continuously supplied with various concentrations ranging from 0 to 20 μM. Prototypes and CadC-T7 biosensors are indicated by open and closed symbols, respectively.

construct synthetic circuits for specific purposes (e.g., biosensors). However, we still lack specific knowledge and/or screening tools that meet the demand for mining useful biological modules from among similar or redundant genes in the databases. Here, we demonstrated how to screen sensory and regulatory bio-parts, including CadC regulators and *cadO* operators, from the genome of a novel bacterial isolate from ocean sediment, and how to obtain proper bio-parts with distinct specificities from among reiterated paralogous genes. Furthermore, we combined T7 signal amplification modules with CadC to generate CadC-T7 synthetic circuits, which were successfully implemented in a microfluidic platform to detect heavy metals with enhanced specificity and sensitivity. Thus, this study shows that combination of the chemostat-like microfluidic platform with newly created microbial genetic circuits synergistically improved the performance of microbial biosensor devices in the detection of heavy metal ions. Our findings illustrate the importance of a convergent approach for the improvement of nano/microbiotechnological biosensor devices.

Conflict of interest statement

The authors have no conflicts of interest to declare.

Acknowledgements

This work was supported by grants from the Next-Generation BioGreen 21 Program (SSAC, PJ01111802 and PJ01118601), Rural Development Administration, and the KRIBB Research Initiative Program, Republic of Korea.

Appendix A. Supplementary material

Supplementary data associated with this article can be found in the online version at http://dx.doi.org/10.1016/j.bios.2015.12.101.

References

Azarbad, H., Niklinska, M., van Gestel, C.A.M., van Straalen, N.M., Roling, W.F.M., Laskowski, R., 2013. Microbial community structure and functioning along metal pollution gradients. Environ. Toxicol. Chem. 32 (9), 1992–2002.
Bereza-Malcolm, L.T., Mann, G., Franks, A.E., 2015. Environmental sensing of heavy metals through whole cell microbial biosensors: a synthetic biology approach. ACS Synth. Biol. 4 (5), 535–546.
Blake, D.A., Jones, R.M., Blake 2nd, R.C., Pavlov, A.R., Darwish, I.A., Yu, H., 2001. Antibody-based sensors for heavy metal ions. Biosens. Bioelectron. 16 (9–12), 799–809.
Cuypers, A., Plusquin, M., Remans, T., Jozefczak, M., Keunen, E., Gielen, H., Opdenakker, K., Nair, A.R., Munters, E., Artois, T.J., Nawrot, T., Vangronsveld, J., Smeets, K., 2010. Cadmium stress: an oxidative challenge. Biometals 23 (5), 927–940.
Dubendorff, J.W., Studier, F.W., 1991. Controlling basal expression in an inducible T7 expression system by blocking the target T7 promoter with lac repressor. J. Mol. Biol. 219 (1), 45–59.
Endo, G., Silver, S., 1995. CadC, the transcriptional regulatory protein of the cadmium resistance system of *Staphylococcus aureus* plasmid pI258. J. Bacteriol. 177 (15), 4437–4441.
Ercal, N., Gurer-Orhan, H., Aykin-Burns, N., 2001. Toxic metals and oxidative stress part I: mechanisms involved in metal-induced oxidative damage. Curr. Top. Med. Chem. 1 (6), 529–539.
Gammoudi, I., Tarbague, H., Othmane, A., Moynet, D., Rebiere, D., Kalfat, R., Dejous, C., 2010. Love-wave bacteria-based sensor for the detection of heavy metal toxicity in liquid medium. Biosens. Bioelectron. 26 (4), 1723–1726.
Garcia-Alonso, J., Greenway, G.M., Hardege, J.D., Haswell, S.J., 2009. A prototype microfluidic chip using fluorescent yeast for detection of toxic compounds. Biosens. Bioelectron. 24 (5), 1508–1511.
Hegab, H.M., Elmekawy, A., Stakenborg, T., 2013. Review of microfluidic microbioreactor technology for high-throughput submerged microbiological cultivation. Biomicrofluidics 7 (2), 21502.
Hobl, B., Hock, B., Schneck, S., Fischer, R., Mack, M., 2013. Bacteriophage T7 RNA polymerase-based expression in *Pichia pastoris*. Protein Expr. Purif. 92 (1), 100–104.
Hou, Q., Ma, A., Wang, T., Lin, J., Wang, H., Du, B., Zhuang, X., Zhuang, G., 2015. Detection of bioavailable cadmium, lead, and arsenic in polluted soil by tailored multiple *Escherichia coli* whole-cell sensor set. Anal. Bioanal. Chem. 407 (22), 6865–6871.
Hurdebise, Q., Tarayre, C., Fischer, C., Colinet, G., Hiligsmann, S., Delvigne, F., 2015. Determination of zinc, cadmium and lead bioavailability in contaminated soils at the single-cell level by a combination of whole-cell biosensors and flow cytometry. Sensors 15 (4), 8981–8999.
Jaishankar, M., Tseten, T., Anbalagan, N., Mathew, B.B., Beeregowda, K.N., 2014. Toxicity, mechanism and health effects of some heavy metals. Interdiscip. Toxicol. 7 (2), 60–72.
Kandegedara, A., Thiyagarajan, S., Kondapalli, K.C., Stemmler, T.L., Rosen, B.P., 2009. Role of bound Zn(II) in the CadC Cd(II)/Pb(II)/Zn(II)-responsive repressor. J. Biol. Chem. 284 (22), 14958–14965.
Kim, M., Lim, J.W., Kim, H.J., Lee, S.K., Lee, S.J., Kim, T., 2014. Chemostat-like microfluidic platform for highly sensitive detection of heavy metal ions using microbial biosensors. Biosens. Bioelectron. 65, 257–264.
Lee, Y.J., Lee, S.J., Jeong, H., Kim, H.J., Ryu, N., Kim, B.C., Lee, H.S., Lee, D.W., Lee, S.J., 2012. Draft genome sequence of *Bacillus oceanisediminis* 2691. J. Bacteriol. 194 (22), 6351–6352.
Lei, Y., Chen, W., Mulchandani, A., 2006. Microbial biosensors. Anal. Chim. Acta 568 (1–2), 200–210.
Lim, J.W., Ha, D., Lee, J., Lee, S.K., Kim, T., 2015. Review of Micro/Nanotechnologies for Microbial Biosensors. Front. Bioeng. Biotechnol. 3, 61.
Nguyen, H.T., Leelavathi, S., Reddy, V.S., 2004. Bacteriophage T7 RNA polymerase-directed, inducible and tissue-specific over-expression of foreign genes in transgenic plants. Plant Biotechnol. J. 2 (4), 301–310.
Nistala, G.J., Wu, K., Rao, C.V., Bhalerao, K.D., 2010. A modular positive feedback-based gene amplifier. J. Biol. Eng. 4, 4.
Raja, C.E., Selvam, G.S., 2011. Construction of green fluorescent protein based bacterial biosensor for heavy metal remediation. Int. J. Env. Sci. Technol. 8 (4), 793–798.
Sayut, D.J., Kambam, P.K., Sun, L., 2007. Engineering and applications of genetic circuits. Mol. Biosyst. 3 (12), 835–840.
Segall-Shapiro, T.H., Meyer, A.J., Ellington, A.D., Sontag, E.D., Voigt, C.A., 2014. A"resource allocator' for transcription based on a highly fragmented T7 RNA polymerase. Mol. Syst. Biol. 10, 742.
Shetty, R.S., Deo, S.K., Shah, P., Sun, Y., Rosen, B.P., Daunert, S., 2003. Luminescence-based whole-cell-sensing systems for cadmium and lead using genetically engineered bacteria. Anal. Bioanal. Chem. 376 (1), 11–17.
Steven, M.P.S., Eric, N.D., Daniel, L.M., Michael, C.H., KY, A.W., N., D., 1996. Comparison of AAs, ICP-AES, PSA, and XRF in determining lead and cadmium in soil. Environ. Sci. Technol. 30 (1), 204–213.
Studier, F.W., 2014. Stable expression clones and auto-induction for protein production in *E. coli*. Methods Mol. Biol. 1091, 17–32.
Sun, Y., Wong, M.D., Rosen, B.P., 2001. Role of cysteinyl residues in sensing Pb(II), Cd (II), and Zn(II) by the plasmid pI258 CadC repressor. J. Biol. Chem. 276 (18), 14955–14960.
Tao, H.C., Peng, Z.W., Li, P.S., Yu, T.A., Su, J., 2013. Optimizing cadmium and mercury specificity of CadR-based *E. coli* biosensors by redesign of CadR. Biotechnol. Lett. 35 (8), 1253–1258.
Temme, K., Hill, R., Segall-Shapiro, T.H., Moser, F., Voigt, C.A., 2012. Modular control of multiple pathways using engineered orthogonal T7 polymerases. Nucleic Acids Res. 40 (17), 8773–8781.
Wang, B., Barahona, M., Buck, M., 2013. A modular cell-based biosensor using engineered genetic logic circuits to detect and integrate multiple environmental signals. Biosens. Bioelectron. 40 (1), 368–376.
Wu, C.H., Le, D., Mulchandani, A., Chen, W., 2009. Optimization of a whole-cell cadmium sensor with a toggle gene circuit. Biotechnol. Prog. 25 (3), 898–903.
Ye, J., Kandegedara, A., Martin, P., Rosen, B.P., 2005. Crystal structure of the *Staphylococcus aureus* pI258 CadC Cd(II)/Pb(II)/Zn(II)-responsive repressor. J. Bacteriol. 187 (12), 4214–4221.